WATER RESOURCES RESEARCH, VOL. 37, NO. 12, PAGES 3265–3273, DECEMBER 2001

Impact of exchange flows on wetland flushing

Hrund Ó. Andradóttir[1] and Heidi M. Nepf

Ralph M. Parsons Laboratory, Department of Civil and Environmental Engineering
Massachusetts Institute of Technology, Cambridge, Massachusetts, USA

Abstract. The flushing of littoral regions is governed by barotropic river flows, Q_R, and baroclinic exchange flows, ΔQ. This note presents field observations of two different flushing regimes in a shallow wetland that borders a lake. In spring, when river flows are high, the wetland circulation is river- or jet-dominated, $\Delta Q/Q_R < 1$, and the river short-circuits through the wetland in a much shorter time than the nominal residence time. During summer low flows, however, the wetland circulation is dominated by exchange flows, $\Delta Q/Q_R > 1$, that vary both on diurnal and synoptic (10–20 days) timescales in response to differential heating and cooling between the wetland and lake and to wind. These exchange flows can enhance wetland flushing by a factor of 10 relative to river flushing. A one-dimensional decoupled heat and flow model represents diurnal exchange flows in this system well and may be used to assess the importance of exchange flows in other systems.

1. Introduction

Littoral regions play an important role in lake water quality. They receive, transform, and conduct nutrients and anthropogenic chemicals from terrestrial systems to lakes. The transport of material through these shallow regions is governed by two major mechanisms: barotropic river flows and baroclinic exchange flows (Figure 1). The exchange flows are generated by differential heating and cooling between regions of different depth or optical clarity and can therefore be highly temporal [*Monismith et al.*, 1990]. Wind can either surpress or promote these flows depending upon the wind direction. For example, winds have been found to increase the flushing of shallow estuaries by a factor of 3 [*Geyer*, 1997].

To date, freshwater exchange flows have been mostly studied in the lab or through numerical modeling. The earlier studies focus on the steady baroclinic circulation in sidearms of cooling lakes and its role in improving heat dissipation [e.g., *Brocard and Harleman*, 1980]. More recent work considers the exchange flows in natural sidearms and characterizes their temporal variability and mixing properties [*Farrow and Patterson*, 1993; *Sturman et al.*, 1996; *Sturman and Ivey*, 1998]. Despite their variability these flows have been found to significantly enhance sidearm flushing [*Sturman et al.*, 1999; *Horsch and Stefan*, 1988] and to contribute to lake nutrient budgets [*James and Barko*, 1991]. Still only very few field observations are available to describe these flows, especially for wide and shallow (<2 m deep) natural sidearms such as wetlands. More importantly, to the authors' knowledge, no study has compared the long-term impact of exchange flows on sidearm flushing to that of river flows. For example, there may be time periods during the year when exchange flows are present but provide no additional flushing because the ratio of exchange flow to river flow is much less than 1.

The goals of this note are to (1) provide field observations of exchange flows between a shallow wetland and a lake, (2) characterize the timescales and magnitudes of the driving forces producing the exchange flows, and (3) evaluate the relative importance of exchange flows to river flows on wetland flushing over the course of a year. The site and study methods are introduced in section 2. The field observations of the meteorological conditions, exchange flows, and wetland circulation are summarized in section 3. Finally, section 4 introduces a simple analytical tool that may be used to assess the importance of exchange flows in other shallow sidearm systems.

2. Methods

2.1. Site

The Upper Mystic Lake is a small (509,000 m^2) dimictic lake located at the base of a contaminated watershed in suburban Boston, Massachusetts (Figure 2a). The Aberjona River delivers nutrients and heavy metals such as arsenic and lead from the watershed to the lake [*Solo-Gabriele and Perkins*, 1997]. Before entering the lake, the river flows through two wetlands, first, the larger upper forebay (140,000 m^2) and then the smaller lower forebay (51,600 m^2). The lake and forebays are surrounded by trees and houses and a hill to the northwest. In this note, we investigate the exchange flow between the lower forebay and the lake that occurs through a 60-m-wide channel which we call the inlet. The lower forebay has a generally flat bathymetry, except for a 2- to 2.4-m-deep channel that runs from the neck toward the lake inlet (dashed line on Figure 2b). Owing to sailing activities the wetland is treated with herbicides every year, leaving only its border and eastern lobe densily vegetated with water lilies and coontail in the summer months. The mean water depth in the wetland ranges from ~1.5 m in late summer to 1.9 m in early spring. The Upper Mystic Lake begins to stratify in April and remains stratified until it overturns in November [*Aurilio et al.*, 1994]. During peak summer stratification the 22°–27°C surface water is separated from the 4°–7°C hypolimnetic water by a 5-m-thick thermocline typically starting at 5–6 m depth. A 1- to 1.5-m-thick diurnal surface heating layer can develop in the lake on warm, calm afternoons.

[1]Now at Mars & Company, Greenwich, Connecticut, USA.

Copyright 2001 by the American Geophysical Union.

Paper number 2001WR000257.
0043-1397/01/2001WR000257$09.00

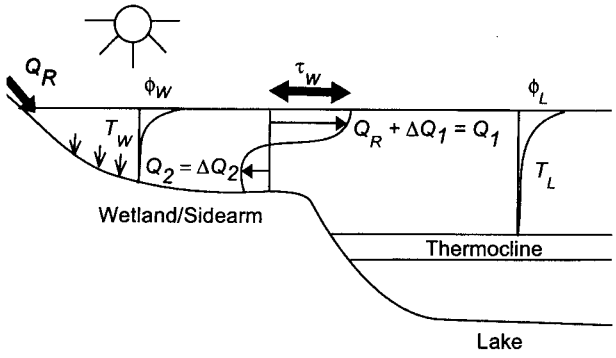

Figure 1. Sidearm flushing is governed by river flows, Q_R, and exchange flows, ΔQ. The exchange flows are generated because of differential heating and cooling between a sidearm and lake ($T_w \neq T_L$) and are modified by wind shear stress, τ_w.

2.2. Observations and Analysis

Two 4-day field studies were conducted in 1997, the first one on April 14–17 during high river flows and the second one at the end of July during low river flows. Water speed and direction were sampled at the inlet at 10- to 30-cm depth intervals (5–7 points in the vertical) three to four times during each study using a Sontek acoustic doppler velocimeter (ADV) with a resolution of 0.1 mm/s. The ADV was deployed from a boat anchored on both ends in April and from a free-standing rod stuck into the wetland sediments in July. The water speed was recorded at each depth for 3–7 min at 12–15 Hz, a long enough record to unambiguously remove surface wave or boat swaying motions. The mobile ADV system was also used to measure the water speeds and directions along the trajectory from the neck to lake inlet (Figure 2b) on April 17 and July 30–31. Hourly Aberjona River flow was measured by the U.S. Geological Survey (USGS) approximately 800 m upstream of the entrance to the upper forebay. A flow rate factor of 1.06 was applied to account for the additional drainage area between the USGS station and the lower forebay. Two independent estimates for the exchange flow rate, ΔQ_1 and ΔQ_2, were derived from each velocity profile at the inlet by calculating the flow rate in the upper and lower layers, Q_1 and Q_2, and then subtracting the river flow rate, Q_R, from the outflowing layer (see Figure 1). The cross-sectional areas of the two layers, A_1 and A_2, and the width of the interface between the layers, w, were estimated from a traverse of depth measurements made across the inlet at 3- to 5-m intervals. The relative magnitude of inertial and buoyant forces was assessed by calculating the composite internal Froude number, G,

$$G^2 = \frac{u_1^2}{g' A_1 / w} + \frac{u_2^2}{g' A_2 / w}, \quad (1)$$

where $u = Q/A$ is the mean water velocity in each layer and $g' = g|\rho_2 - \rho_1|/\rho$ is the reduced gravity based upon the density in the upper and lower layers, ρ_1 and ρ_2 [*Dalziel*, 1992]. Tracer experiments were also conducted, in which 25 g and 39 g of Rhodamine WT dye were released across the width of the neck over a 20-min interval on April 17 (10:20 A.M.) and on July 30 (12:35 P.M.), respectively. The dye leaving the wetland was monitored over the first several hours following the release by measuring vertical profiles of dye and temperature with vertical resolution of 2–5 cm at three different locations across the lake inlet. In addition, fluorometer and

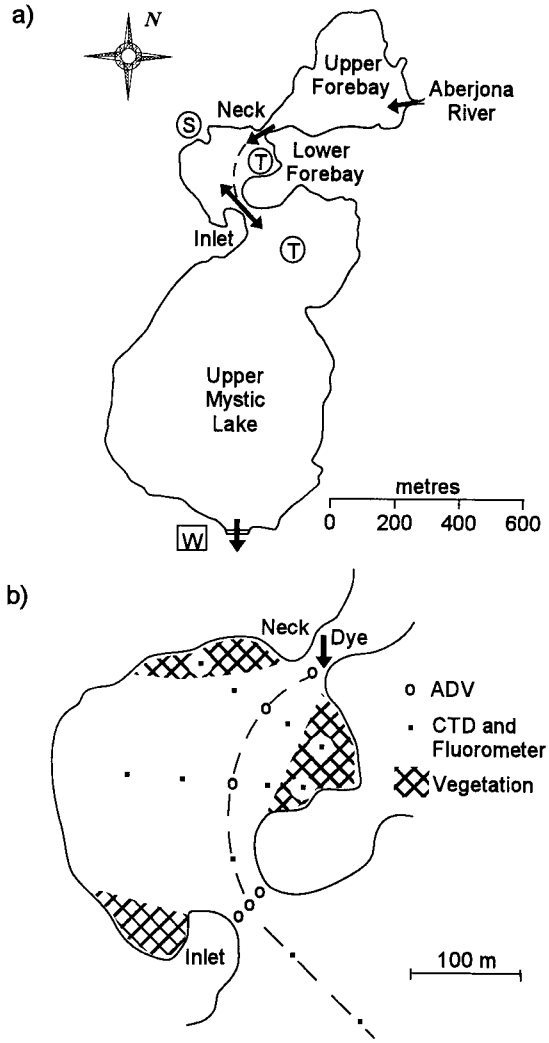

Figure 2. (a) The Upper Mystic Lake system field site and monitoring program. Exchange flows occur at the inlet between the lower forebay and lake. Locations of water temperature probes are denoted by T, anemometer is denoted by W, and the weather station is denoted by S. (b) A close-up on the lower forebay, with locations of the acoustic doppler velocimeter (ADV) and conductivity-temperature-depth (CTD) vertical profiles (July study).

conductivity-temperature-depth (CTD) profiles were taken inside the wetland and the lake on April 16 (9:00–10:00 A.M., 11:00 A.M. to 1:00 P.M.), April 17 (9:00–10:00 A.M.), July 30 (1:00–2:00 P.M., 3:00 P.M., and 6:00 P.M.), July 31 (11:30 A.M. to 1:00 P.M., 5:30–6:30 P.M.) and August (4:00–5:00 P.M.). A map of typical fluorometer and CTD measurement locations is portrayed on Figure 2b. A Differential Global Positioning System provided 3- to 5-m accuracy on spatial position.

In addition to the two field experiments, air temperature, relative humidity, and solar radiation were monitored every 5 min in the lower forebay from April through November 1997. Simultaneously, wind speed, W_{10}, and direction, θ, were measured 10 m above ground at an unobstructed location at the southern end of the lake at 10-min intervals. The measured wind represents well the conditions over the lake. The inlet and wetland, however, may experience significant wind sheltering

relative to the lake because of a nearby hill and surrounding houses and trees. The net heat fluxes over the lake were calculated from these measurements and cloud cover monitored at the Boston Logan Airport (15 km east of the study site) using established empirical relationships [*e.g., Fisher et al.*, 1979, p. 163]. Continuous records of water temperature were also taken at 5-min intervals during the fall of 1997 in the lower forebay both 10–20 cm below the surface and 10–20 cm above the bed using Onset temperature loggers with 0.2°C resolution and at 1-m intervals in the shallower northern region of the lake using thermistor chains with 0.1°C resolution [*Fricker and Nepf*, 2000] (T on Figure 2a). On the basis of vertical temperature profiles in this system the depth-averaged wetland temperature was found to be best represented as the weighted average of the continuous surface (67%) and near-bed (33%) temperatures. Similarly, the water temperature recorded continuously at 1.8 m depth was found to most closely represent the depth-averaged water temperature in the lake epilimnion (top 5 m). The longitudinal density gradient from the wetland into the lake, $\partial\rho/\partial x$, was calculated based upon the depth-averaged temperature difference between the lake surface and wetland waters, $\Delta\rho = \rho|_{T_L} - \rho|_{T_W}$, and the length scale for the longitudinal temperature gradient, Δx. Detailed CTD profiling along the transect from the wetland into the lake indicated that 80–90% of the temperature drop occurred within 100 ± 30 m of the inlet, so Δx was chosen as 100 m. The longitudinal gradient Wedderburn number,

$$We_g = \frac{g\,\frac{\partial \rho}{\partial x}\,H_{\max}^2}{\tau_w}, \tag{2}$$

was used to estimate the relative importance of buoyancy and wind stress in generating the exchange flows within the inlet channel with maximum depth, $H_{\max}$. The mean wind stress, τ_w, along the direction of the flow axis (wetland to lake), θ_x, was estimated as

$$\tau_w = \rho_a C_{10} W_{10}^2 \cos(\theta - \theta_x), \tag{3}$$

where ρ_a is the air density and $C_{10} = 10^{-3}$ is the wind drag coefficient [*Hicks et al.*, 1974]. Last, an opposing wind balances the buoyant forcing and produces minimum steady exchange flows when $We_g \approx -(7\text{–}9)$ [*Andradóttir*, 2000]. On this basis the criterion for which the wind dominates buoyancy was taken as

$$|We_g| \lesssim 8. \tag{4}$$

The sign of the We_g was used to determine whether the wind promoted ($We_g > 0$) or surpressed ($We_g < 0$) the density-driven circulation.

3. Results

3.1. Meteorological Conditions

As discussed in section 1, the two major flushing mechanisms in lake sidearms are river throughflows and exchange flows driven by differential heating and cooling and modified by winds. Figure 3 summarizes the variation in the meteorological conditions controlling these flushing mechanisms in the Upper Mystic Lake wetland system. First, consider the 10-day average Aberjona River flow rate. Figure 3a shows that the river flow changes drastically over the course of the year from approximately 2 m^3/s during spring surface runoff and snowmelt to 0.1 m^3/s and less during the dry summer. This strong seasonal variation in the Aberjona River flow is typical of many rivers in temperate regions.

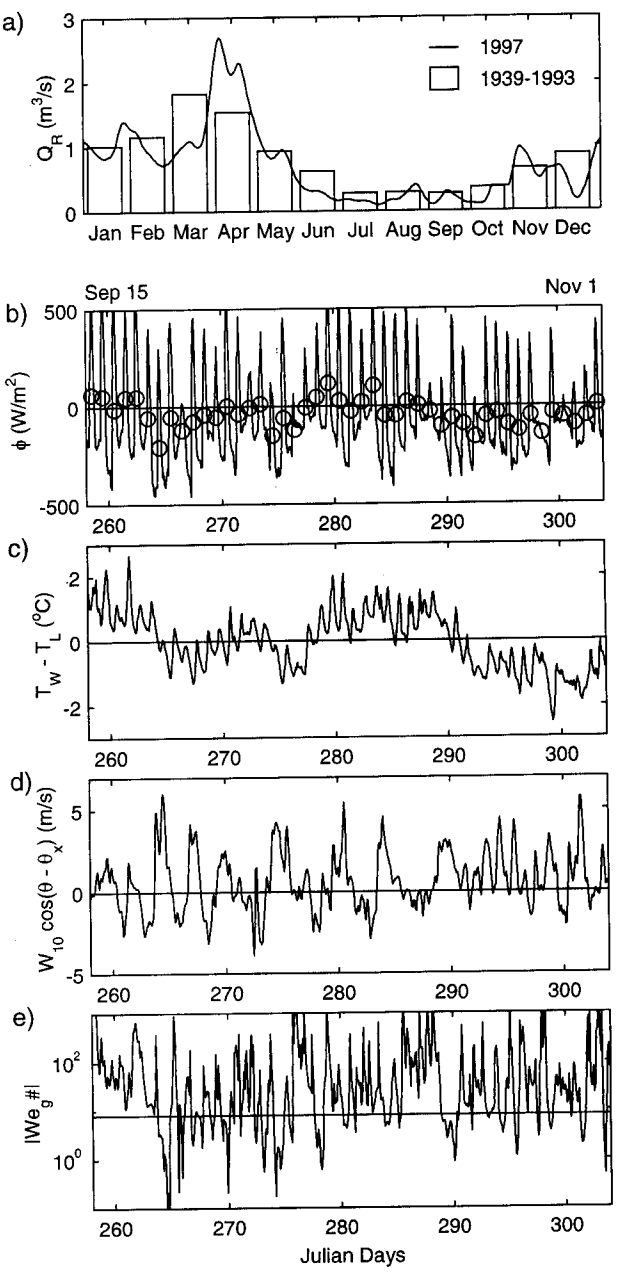

Figure 3. Meteorological conditions in the Upper Mystic Lake system. (a) Aberjona River flow rates. (b) Instantaneous (solid lines) and daily (circles) net surface heat fluxes per unit area. (c) Difference between the weighted average of surface and near-bed water temperature in the wetland, T_W, and the temperature at 1.8 m depth in the lake, T_L. (d) Mean wind speeds along inlet axis (positive wind is into lake). (e) Wedderburn numbers. For clarity, the records have been low-pass filtered using a second-order Butterworth filter with cutoff frequency of 0.1 cpd and 0.5 cph.

In contrast to the river flow, differential heating and cooling between a wetland and lake occurs predominantly on shorter timescales than a year [*Andradóttir and Nepf*, 2000]. This is particularly the case for wetlands that exchange with a lake much faster than annually and thus mimic the lake annual

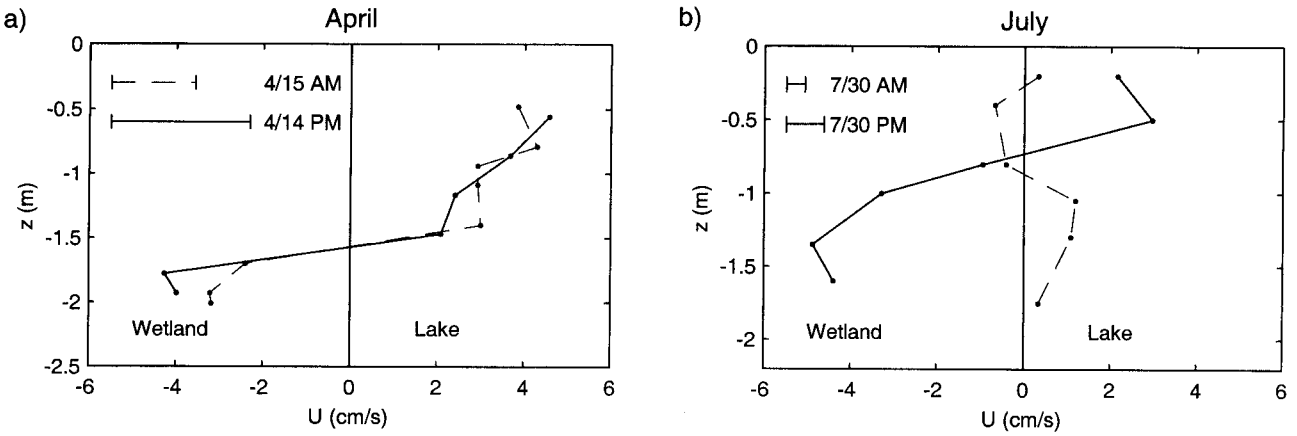

Figure 4. Average water speeds based on 3- to 7-min records at the center of the inlet between the wetland and lake in (a) April and (b) July 1997. The horizontal bars represent 1 standard deviation around the mean speed, after removing motions associated with boat sway, and are mostly an indication of water turbulence levels.

heating cycle. The close-up in Figure 3b shows the net surface heat fluxes over the Upper Mystic Lake during a typical low flow period in fall, when $Q_R < 0.4$ m^3/s. The surface heat fluxes vary considerably over the course of the day and from day to day as shown by the net daily heat fluxes (circles). This produces both diurnal and synoptic (10–20 days) differential heating and cooling, where the wetland water oscillates from being 1°–2°C warmer to 1°–2°C colder than the lake surface waters (Figure 3c). Notice that the synoptic variations can exceed the diurnal variations, for example, during J.D. = 280–300. This strong synoptic component, to the authors' knowledge, has not been previously reported in sidearm literature.

Last, winds over the Upper Mystic Lake blow predominantly from the south at 1.4–2 m/s in summer and from the north at 1.8–3 m/s in spring and fall. A close-up on a 1.5-month fall period (Figure 3d) reveals that the wind component along the inlet from the wetland into the lake typically changes direction every 1–3 days and can vary in speed anywhere from 0–6 m/s over the course of one to several days. Therefore, as with differential heating and cooling, winds vary mostly on synoptic and diurnal timescales. The influence of wind on density-driven flows can be evaluated with a time series of the longitudinal Wedderburn number, We_g. Figure 3e illustrates $|We_g|$ derived from the wind and temperature measurements in Figures 3c and 3d. The elongated time periods for which $|We_g| < 8$ indicate that the wind is an important mechanism in modifying baroclinic exchange flows in this system. During these time periods the sign of the We_g varies mostly on 1- to 3-day timescales, as a result of changing wind directions (Figure 3d) given the strong synoptic variability in temperature variations (Figure 3c). Accounting for this variability in the sign of We_g, (4) suggests that the wind suppresses the density-driven circulation 10–25% of the time and promotes it 5–12% of the time during this fall period. These percentage ranges were calculated by considering the uncertainty in the Wedderburn number, originating both from the uncertainty in estimating the density gradients (33%) and the local wind stress along the lake inlet into the wetland (20%). The latter uncertainty is largely associated with projecting the wind from the southern end of the lake to the lake inlet. The formulation (3) does not account for wind sheltering, such that northerly winds (short fetch) may be overestimated. Last, since monthly average wind speeds are fairly constant throughout the year in this system, winds are expected to play an equally significant role in modifying the baroclinic circulation during other seasons not shown in Figure 3e.

3.2. Inlet Flow Characteristics

As shown in Figure 3, river flows vary predominantly on seasonal timescales, whereas freshwater exchange flows are largely forced on synoptic and diurnal timescales. This section provides water current observations that support these timescales of variability and indicate how important exchange flows can be relative to river flows for wetland flushing.

Figures 4a and 4b illustrate morning (dashed lines) and afternoon (solid lines) water speed profiles at the center of the inlet during the spring (high river flow) and summer (low river flow) studies, respectively. These centerline flow speeds are representative of the flow across the entire cross section based on additional profiles taken to the left and right of the centerline. In the April study the wetland and lake water are both warming, and the wetland is persistently 1°–1.7°C warmer than the lake surface water. Consistent with this, a sustained two-layered flow is observed in the afternoon of April 14 (solid line on Figure 4a), with the warmer wetland water moving toward the lake at the surface at 4 cm/s and bottom water entering from the lake at 3 cm/s. During the following morning (dashed line on Figure 4a) the same flow pattern is maintained during slightly less windy conditions. Again 2 days later, this flow pattern is observed both at the western and eastern side of the inlet (not shown on Figure 4a). In July, however, the flow along the inlet varies significantly over the course of the day. Specifically, Figure 4b shows that at 10:00 A.M. in the morning on July 30, when the wetland bottom water is 0.2°C colder than the lake surface layer, a weak (<1.5 cm/s) two-layered flow occurs, with bottom outflow from the wetland and a surface intrusion from the lake. In the midafternoon of that same day, by which time the wetland water has become 0.8°C warmer than the lake water, the flow has reversed direction and become much stronger (>4 cm/s) since the morning. A similar afternoon velocity profile was observed at three different locations across the lake inlet the following day (not shown on Figure 4b). The diurnal flow reversal in July and the sustained

Table 1. Exchange Flow Characteristics at Lake Inlet and Daily Wind During the 1997 April and July Studies[a]

Date	Time, LT	W_{10}, m/s	Wind Direction	Q_1, m^3/s	Q_2, m^3/s	ΔQ_1, m^3/s	ΔQ_2, m^3/s	Q_R, m^3/s	$\Delta Q/Q_R$	G^2
April 14	2:00 P.M.	5.3 ± 2.1	NW	2.4	−0.4	0.2	0.4	2.2	0.1–0.2	3
April 15	10:00 A.M.	2.7 ± 1.6	NW	2.2	−0.3	0.4	0.3	1.8	0.2	3
April 17	1:30 P.M.	0.8 ± 0.5	S	1.5	−0.1	0	0.1	1.5	0.1	6
July 25	12:40 P.M.	5.1 ± 1.3	NE	−0.2	0.3	0.2	0.2	0.09	2	0.3
July 30	10:20 A.M.	2.9 ± 1.1	N	−0.1	0.2	0.1	0.1	0.06	2	0.0
July 30	3:40 P.M.	2.9 ± 1.1	N	0.6	−0.9	0.5	0.9	0.06	8–15	0.7
July 31	2:20 P.M.	1.7 ± 0.8	NW	0.9	−0.8	0.8	0.8	0.06	13	0.7

[a]The positive sign corresponds to the wetland outflow to the lake, and the negative sign corresponds to the return flow from the lake into the wetland. The accuracy of the flow rate estimates is 25%, which incorporates a 10% uncertainty in cross-sectional area, a 10%–15% uncertainty in the mean of the vertical speed profile, and a 6–10% uncertainty in the expansion of this profile across the cross section.

April flows reflect the diurnal and synoptic timescales for differential heating and cooling discussed in section 3.1.

Let us now take a closer look at the magnitude of the two major flushing mechanisms in the wetland. Table 1 summarizes both the measured Aberjona River flow rates, Q_R, and the estimated exchange flow rates, $\Delta Q_{1,2}$ (see section 2.2), at various times during the two study periods. Table 1 shows that the exchange flows are of the same order of magnitude during both studies, consistent with the observation that the driving forces, buoyancy and wind, do not vary significantly with season (section 3.1). The good agreement between the two independent estimates of the exchange flows, ΔQ_1 and ΔQ_2, is an indication of measurement accuracy. The Aberjona River flows, however, are ~20 times larger during the spring study than the summer study. This leads to a shift in wetland flushing regime. In spring the river is the dominant flushing mechanism, $\Delta Q/Q_R < 0.2$, whereas in summer the exchange flows become the dominant flushing mechanism, $\Delta Q/Q_R = 2$–15. Sections 3.3 and 3.4 consider how this shift affects wetland circulation and flushing timescales.

3.3. Wetland Circulation

A change in $\Delta Q/Q_R$ implies a shift in wetland circulation. In spring, when the circulation is river-dominated, $\Delta Q/Q_R < 1$, the flow at the lake inlet is supercritical based on $G^2 > 1$ in Table 1. The dominance of inertial forces causes the river to behave like a jet, which independent of the wind and buoyancy takes the shortest path across the wetland (Figure 5a). In summer, however, the wetland circulation is exchange-dominated, $\Delta Q/Q_R > 1$, with buoyancy and wind as the main driving forces. Since the buoyancy forcing results from differential heat absorption between the wetland and lake, it acts on the whole wetland. Consequently, this forcing is expected to produce a point sink at the lake inlet, with water drawn from all directions, as illustrated on the schematic Figure 5b. In the case of nonuniformly vegetated wetlands the flow will draw preferentially from sparsely vegetated areas that offer the least flow resistance.

Water speed and temperature measurements in the wetland support the different circulation patterns described above. Figure 5c shows that in April the current speeds slowly decrease along the trajectory from the neck to the lake inlet, consistent with a river jet entraining water while it crosses the wetland. Toward the neck ($x < 100$ m) the warm river jet occupies all of the water column, as seen by the unidirectional flow. The cold return flow from the lake is arrested halfway into the wetland, consistent with $G^2 > 1$ (Table 1), and *Dalziel*'s [1992] hydraulic control theory, which predicts that the high spring flow rates severely constrain or even fully arrest the exchange flow. In July, however, the wetland surface and bottom current speeds increase toward the inlet (Figure 5d). Since the water depth is also increasing, this acceleration suggests that the wetland inflow and outflow are tunneled from a wide portion of the wetland through the narrow channel to the lake as schematically illustrated on Figure 5b. At the inlet constriction the flow is subcritical, $G^2 < 1$ (Table 1), suggesting that summer exchange flows in the Upper Mystic Lake are submaximal. This is also consistent with *Dalziel*'s [1992] hydraulic control theory, which predicts maximal flow rates of 0.6–1.2 m^3/s that generally exceed the observed flow rates at the lake inlet (Q_1 and Q_2 in Table 1). Figure 5d also shows that the exchange flow extends from the lake across the wetland and even up into the upper forebay, as displayed by the upstream bed velocity measured near the neck. The surface water temperatures are gradually cooling from 27°C at the neck to 25°C at the lake inlet. This suggests a continuous entrainment of colder water from the lower layer, similar to the sidearm circulation observed by *Adams and Wells* [1984] and modeled, for example, by *Jain* [1980].

3.4. Wetland Flushing

In the previous section the wetland circulation was shown to change from jet flow in spring (Figure 5a) to point sink flow in the summer and fall (Figure 5b). This change also affects the flushing dynamics of the wetland. To evaluate the flushing timescales and provide additional support to the circulation described above, a slug of dye was released at the neck, and the dye concentrations were monitored at the lake inlet. The results are shown on Figures 5e and 5f.

In April a substantial portion (20%) of the dye mass exits the wetland in only 2.5 ± 0.3 hours (Figure 5e). This is much shorter than the nominal residence time of 18 hours, defined as the ratio between the wetland volume and total flow

$$t_{\text{nom}} = \frac{AH}{Q_R + \Delta Q}. \tag{5}$$

This short circuiting is consistent with a jet-dominated circulation (Figure 5a). Furthermore, the observed short-circuiting timescale of 2.5 hours corresponds closely with what shallow jet theory predicts for the Upper Mystic Lake site configuration [*Chu and Baines*, 1989]. Also note that during the short-circuiting period, higher dye concentrations occur at the western side of the inlet (circles on Figure 5e) than at the center and eastern side (solid lines and crosses), consistent with a linear jet trajectory between the wetland entrance and the lake (Figure 5a).

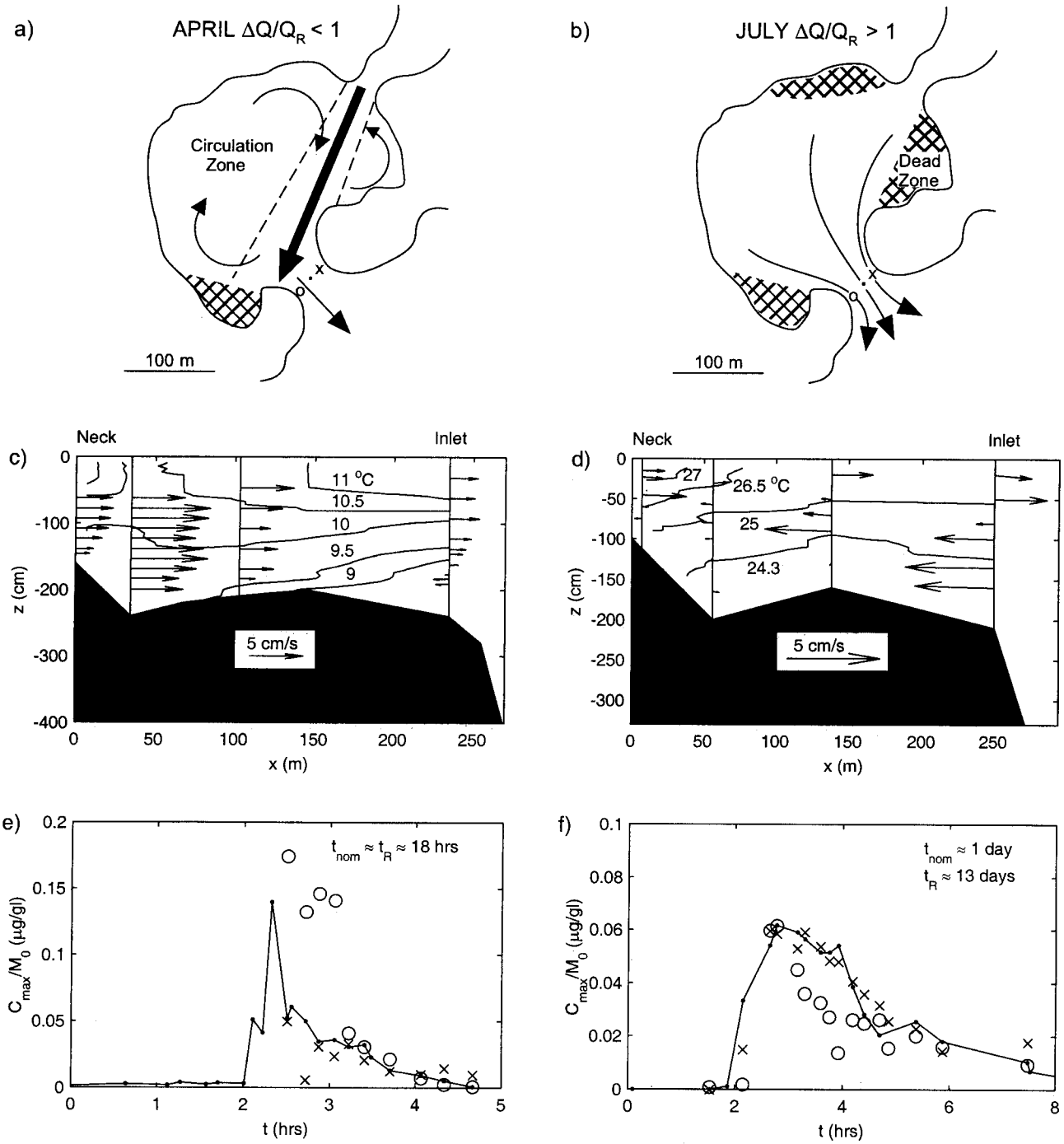

Figure 5. Wetland circulation and flushing regimes. Schematic of the (a) jet-dominated circulation in spring and (b) point sink circulation in summer (and fall). Longitudinal temperature and speed transect from the neck to the lake inlet (c) on April 16 (11:00 A.M. to 1:00 P.M.) and April 17 (8:00 A.M. to 2:00 P.M.), respectively, and (d) on July 30 (noon to 1:00 P.M.) and July 31 (11:00 A.M. to 4:00 P.M.), respectively. Maximum dye concentrations measured over depth at the west (circles), center (solid lines), and east (crosses) side of the inlet normalized by the injected mass, M_0, following the slug releases on (e) April 17 (10:20 A.M. to 3:20 P.M.) and (f) July 30 (12:30–8:30 P.M.).

In July, however, Figure 5f shows that it takes approximately 3 times as long (8 hours) for a similar portion (30%) of the injected dye mass to leave the wetland. In addition, the highest dye concentrations occur persistently at the center and eastern side of the lake inlet. Both of these observations are consistent with the point sink circulation depicted in Figure 5b. Unlike April, the nominal flushing timescale of the wetland cannot be estimated from (5) because ΔQ varies with time during the summer study, often reversing at night as discussed in section 3.2. During such unsteady flow conditions the nominal flushing timescale, t_{nom}, or the timescale for net transport of material through the wetland to the lake, can be assessed from the

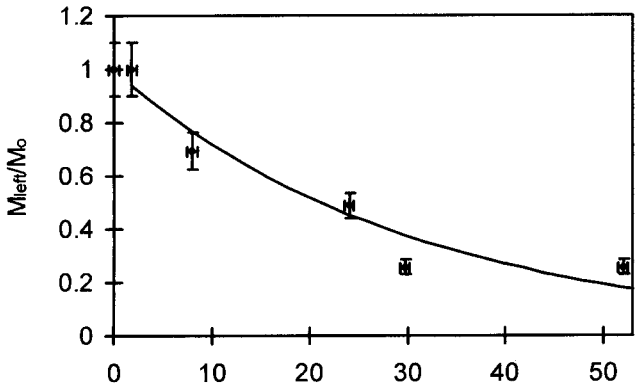

Figure 6. Fraction of mass retained in the wetland after the July 30 dye release, based on dye and flow measurements at the lake inlet ($t < 8$ hours), and dye concentration measurements at 6–15 locations in the wetland ($t > 8$ hours).

decay of dye mass left in the wetland, $M_{\text{left}}(t)$, relative to the injected mass, M_0,

$$t_{\text{nom}} = \frac{\int_0^\infty M_{\text{left}}(t)\, dt}{M_0} \approx \frac{\sum M_{\text{left}} \Delta t}{M_0}. \tag{6}$$

Figure 6 displays the mass of dye left in the wetland following the July slug release, estimated from cumulative outflow (for $t < 8$ hours) and from concentration measurements within the wetland (for $t > 8$ hrs). For these measurements, (6) yields an effective wetland flushing timescale of 1.0 ± 0.1 days. Alternatively, assuming a stirred reactor and fitting the measurements on Figure 6 to an exponential decay curve gives $\bar{t}$ = 1.2 ± 0.1 days, which compares within the uncertainty to the previous estimate. Equating (5) with the results of (6) indicates that the unsteady exchange flow produces flushing equivalent to an effective steady exchange flow rate, ΔQ, of 0.6 m^3/s. This value corresponds closely to the maximum exchange flow observed during this study (Table 1), suggesting that the exchange flow contributes efficiently to the net flushing of the wetland, with little mass returning when the flow reverses.

The significance of the exchange flows on wetland flushing is shown by comparing the observed nominal flushing timescale (6) to the nominal flushing timescale due to river flows only ((5) with $\Delta Q = 0$ and Q_R from Table 1), that is,

$$t_R = \frac{AH}{Q_R} = \frac{51{,}600 \times 1.3 \text{ m}^3}{0.06 \text{ m}^3/\text{s}} = 13 \pm 1 \text{ days}.$$

That $t_{\text{nom}} \ll t_R$ demonstrates that exchange flows can significantly enhance wetland flushing, specifically in this system by a factor of 10. With this dramatically enhanced flushing the capacity of the wetland to remove contaminants and thermally mediate the temperature of the lake inflow is impaired. Consequently, wetlands that exchange with lakes play a very different role in lake water quality than wetlands that do not exchange with lakes. Specifically, instead of being considered as transformers, they need to be considered as "communicators" in the sense that they communicate properties from the shoreline (e.g., watershed runoffs) to the lake interior. This communication capacity will be reduced if these littoral regions are very densely vegetated, because of the drag imposed on the flow by the plants.

4. Discussion

The observations in the Upper Mystic Lake system demonstrate two different circulation and flushing regimes. In spring, when river flow rates are high, the circulation is river- or jet-dominated, whereas in summer the circulation is exchange-dominated. Many wetland-lake systems follow similar seasonal trends in atmospheric heating and river flow rates as the one studied in this note and could go through a similar transition. Therefore it is useful to derive an expression for the magnitude of the exchange flows based on readily available information such as site geometry and meteorological conditions. This allows us to assess the potential importance of exchange flows prior to undertaking field experiments and can help guide future studies. Building upon the work of *Farrow and Patterson* [1993], we will make several simplifying assumptions to find an analytical solution for the exchange flow rates and later discuss the limitations of those assumptions. Let us start by considering the heat budget. The one-dimensional governing equation for the mean water temperature, T, can be written as

$$\frac{\partial T}{\partial t} + u\frac{\partial T}{\partial x} = \frac{\phi}{\rho C_p h}, \tag{7}$$

where $u(z)$ is the water speed associated with the exchange flows, ϕ is the net heat flux per surface area assumed to be uniformly distributed over depth h, and ρ and C_p are the density and specific heat of water, respectively. Note that h is typically limited by the water depth in shallow sidearms and the light absorption depth (Secchi depth) in deeper lakes. To decouple the thermal and momentum equations, we start by setting aside the advective heat flux term $u\ \partial T/\partial x$. Differentiating the simplified version of (7) along the flow axis, x, yields the following governing equation for the longitudinal temperature gradient:

$$\rho C_p \frac{\partial}{\partial t}\left(\frac{\partial T}{\partial x}\right) = \frac{1}{h}\left(\frac{\partial \phi}{\partial T}\frac{\partial T}{\partial x} + \frac{\partial \phi}{\partial W_{10}}\frac{\partial W_{10}}{\partial x} + \frac{\partial \phi}{\partial S}\frac{\partial S}{\partial x}\right) - \frac{\phi}{h^2}\frac{\partial h}{\partial x}. \tag{8}$$

The first term on the right-hand side of (8) represents the feedback of the temperature gradient on surface heating which is generally neglected. The next two terms correspond to wind sheltering and sun shading, both of which can be important in small littoral wetlands surrounded by obstructions such as hills, trees, and buildings. In practice, however, estimating these terms is difficult as it requires detailed spatial measurements of both wind speeds, W_{10}, and incoming solar radiation, S. The remaining term describes differential heat absorption and is typically the biggest contributor to differential heating and cooling. Therefore it is the sole term that will be kept in the following analysis. Assuming that the net surface heat flux varies sinusoidally with period, P, and amplitude, $\Delta\phi$,

$$\phi = \Delta\phi e^{i2\pi t/P}, \tag{9}$$

and plugging (9) into (8) gives an estimate for the temperature gradient amplitude as

$$\left|\frac{\partial T}{\partial x}\right| \approx \frac{\Delta\phi P}{2\pi\rho C_p h^2}\left|\frac{\partial h}{\partial x}\right|. \tag{10}$$

Similarly, but not shown, assuming that the flow is viscous-dominated and at a quasi steady state with the pressure gra-

dient, the exchange flow rates associated with differential heating and cooling can be derived as

$$\Delta Q = 5.4 \times 10^{-3} \frac{g\alpha \left| \frac{\partial T}{\partial x} \right| AH^3}{K_{mz}}, \quad (11)$$

where g is the acceleration of gravity, $\alpha = (1\text{–}2)10^{-4}$/°C is the thermal expansivity, K_{mz} is the vertical diffusivity of momentum, and A and H are the cross-sectional area and depth at the sidearm/wetland entrance, respectively [*Andradóttir*, 2000]. Replacing $\alpha\ \partial T/\partial x$ with $\partial\rho/\partial x$, this solution corresponds to the widely used *Hansen and Rattay* [1965] and *Officer* [1976, p. 118] model for estuarine baroclinic circulation. Incorporating (10) into (11), the magnitude of the exchange flows can be compared to the river flows to determine whether and when density-driven exchange flows contribute significantly to sidearm flushing. Similarly, plugging (10) into the Wedderburn number (2) determines the potential effects of winds in modifying freshwater exchange flows.

For validation this analysis is used to predict the diurnal temperature gradient and exchange flow rates in the Upper Mystic Lake system. During summer and fall, Figure 3b shows daily (P = 1 day) heat flux variations with amplitude $\Delta\phi$ = 300–400 W/m^2. Recall from section 2.2 that $\Delta\phi$ can be estimated based on solar radiation, wind speed, cloud cover, air temperature, relative humidity and water temperature measurements, the majority of which are available from local weather services. The heat absorption gradient, $|\partial h/\partial x|$, is 0.04 m/m based on the bottom slope along the lake inlet with 60–70 m^2 cross-sectional area and 2.5 m maximum depth. The same gradient can be derived from the difference between the mean wetland water depth (1.5 m) and lake epilimnion depth (5 m) over the inlet length (~100 m). With this input, (10) yields $|\partial T/\partial x| \approx 0.007$°C/m which compares within 10–20% to our observed amplitude of diurnal temperature variations (~1°C on Figure 3c) over a length of 100 ± 30 m. On the basis of microstructure temperature measurements at this site [*Nepf and Oldham*, 1997], $K_{mz} = O(10^{-4}$ m^2/s), for which (11) yields an exchange flow rate of

$$\Delta Q \approx 5.4 \times 10^{-3} \frac{9.8 \times 1.5 \times 10^{-4} \times 0.007 \times 65 \times 2.5^3}{10^{-4}}$$

$$\approx 0.6 \text{ m}^3/\text{s},$$

which agrees within the uncertainty of measurements with the observed maximum flow rates during the July study (Table 1). Thus despite the simplifying assumptions, (10) and (11) represent well the diurnal exchange flow in the Upper Mystic Lake system, indicating they may be a useful prediction tool, especially in situations when resources are not available to conduct an intense field program.

Finally, let us reconsider some of the assumptions made to obtain the simple analytical expressions (10) and (11). For a start, the analysis neglects the heat fluxes associated with the exchange flows. While the advective heat fluxes are not insignificant, they do not drastically modify the density gradients in a sidearm that is flushed out at a similar or lower rate than the rate of heating/cooling. However, if the sidearm is flushed out faster than the timescale for heating/cooling, advective flows play a significant role mediating the density gradient. For example, in the Upper Mystic Lake sidearm system, which is flushed out diurnally, (10) significantly overestimates the density gradient associated with synoptic (P = 10–20 days) heating/cooling. Therefore (10) and (11) are not representative for the synoptic flow variability at that site, and to predict those flows, the coupled thermal and flow equations must be solved numerically. The model also assumes that the flow is at quasi steady state and is viscous-dominated. Both assumptions hold reasonably well in shallow sidearms with a mild density gradient such as wetlands (based on *Farrow and Patterson* [1993] and *Monismith et al.* [1990]). Also note that the model presented here depends strongly on K_{mz}, which may vary during the day as the exchange flow progresses and with variable wind conditions. To the authors' knowledge, no work has been done to parameterize K_{mz} in terms of the flow conditions in shallow freshwater systems, so K_{mz} may ultimately need to be measured at each site using, for example, a microstructure temperature profiler. Last, our model does not account for bed friction and thus will overestimate flows in densely vegetated systems.

To conclude, this note presents field observations in a wetland-lake system that highlight the importance of exchange flows to wetland flushing and the seasonal variation of their importance. Specifically, during high spring flows the river dominates the wetland flushing, whereas in the dry summer, exchange flows can enhance wetland flushing by a factor of 10 relative to river flushing. A one-dimensional decoupled heat and flow model is found to predict well the magnitude of diurnal exchange flows in the Upper Mystic Lake sidearm system, indicating that it can be a valuable tool for first-order assessment of the importance of exchange flows in other shallow freshwater sidearms.

Acknowledgments. This work was funded by the National Institute of Environmental Health Sciences, Superfund Basic Research Program, grant P42-ES04675. The authors would like to thank Rocky Geyer for his valuable insight; David Senn, Harry Hemond, and Terry Donohue for their help in designing the field studies; David Senn, Wendy Pabich, Katja Knauer, Jenny Jay, Dan Brabander, Carolyn Oldham, Kathryn Linge, Chrissy Reilly, Marnie Bell, Shu-Fen Yun, and Daniel Feller for their fieldwork participation. Special thanks go to the Winchester and Medford boat clubs for facilitating our field data collection.

References

Adams, E. E., and S. A. Wells, Field measurements on side arms of Lake Anna, VA, *J. Hydraul. Eng.*, *110*(6), 773–793, 1984.

Andradóttir, H. Ó., Littoral wetlands and lake inflow dynamics, Ph.D. thesis, Mass. Inst. of Technol., Cambridge, 2000.

Andradóttir, H. Ó., and H. M. Nepf, Thermal mediation by littoral wetlands and impact on intrusion depth, *Water Resour. Res.*, *36*(3), 725–735, 2000.

Aurilio, A. C., R. P. Mason, and H. F. Hemond, Speciation and fate of arsenic in three lakes of the Aberjona Watershed, *Environ. Sci. Technol.*, *28*, 577–585, 1994.

Brocard, D. N., and D. R. F. Harleman, Two-layer model for shallow horizontal convective circulation, *J. Fluid Mech.*, *100*, 120–146, 1980.

Chu, V. H., and W. D. Baines, Entrainment by buoyant jet between confined walls, *J. Hydraul. Eng.*, *115*(4), 475–492, 1989.

Dalziel, S. B., Maximal exchange in channels with nonrectangular cross section, *J. Physical Oceanogr.*, *22*, 1188–1206, 1992.

Farrow, D. E., and J. C. Patterson, On the response of a reservoir sidearm to diurnal heating and cooling, *J. Fluid Mech.*, *246*, 143–161, 1993.

Fisher, H. B., E. J. List, R. C. Y. Koh, J. Imberger, and N. H. Brooks, *Mixing in Inland and Coastal Waters*, Academic, San Diego, Calif., 1979.

Fricker, P. D., and H. M. Nepf, Bathymetry, stratification, and internal seiche structure, *J. Geophys. Res.*, *105*(C6), 14,237–14,251, 2000.

Geyer, R. W., Influence of wind on dynamics and flushing of shallow estuaries, *Estuarine Coastal Shelf Sci.*, *44*, 713–722, 1997.

Hansen, D. V., and M. Rattay Jr., Gravitational circulation in straits and estuaries, *J. Marine Res.*, *23*, 104–122, 1965.

Hicks, B. B., R. L. Drinklow, and G. Grauze, Drag and bulk transfer coefficients associated with a shallow water surface, *Boundary Layer Meteorol.*, *6*, 287–297, 1974.

Horsch, G. M., and H. G. Stefan, Convective circulation in littoral water due to surface cooling, *Limnol. Oceanogr.*, *33*(5), 1068–1083, 1988.

Jain, S. C., Density currents in sidearms of cooling ponds, *J. Energy Div. Am. Soc. Civ. Eng.*, *106*(EY1), 9–21, 1980.

James, W. F., and J. W. Barko, Estimation of phosphorus exchange between littoral and pelagic zones during nighttime convective circulation, *Limnol. Oceanogr.*, *36*(1), 179–187, 1991.

Monismith, S. G., J. Imberger, and M. L. Morison, Convective motions in the sidearm of a small reservoir, *Limnol. Oceanogr.*, *35*(8), 1676–1702, 1990.

Nepf, H. M., and C. E. Oldham, Exchange dynamics of a shallow contaminated wetland, *Aquat. Sci.*, *59*, 193–213, 1997.

Officer, C. B., *Physical Oceanography of Estuaries (and Associated Coastal Waters)*, John Wiley, New York, 1976.

Solo-Gabriele, H., and F. Perkins, Watershed-specific model for streamflow, sediment and metal transport, *J. Environ. Eng.*, *123*(1), 61–70, 1997.

Sturman, J. J., and G. N. Ivey, Unsteady convective exchange flows in cavities, *J. Fluid Mech.*, *368*, 127–153, 1998.

Sturman, J. J., G. N. Ivey, and J. R. Taylor, Convection in a long box driven by heating and cooling on the horizontal boundaries, *J. Fluid Mech.*, *310*, 61–87, 1996.

Sturman, J. J., C. E. Oldham, and G. N. Ivey, Steady convective exchange flows down slopes, *Aquat. Sci.*, *61*, 260–278, 1999.

H. M. Nepf, Ralph M. Parsons Laboratory, Department of Civil and Environmental Engineering, Room 48-423, Massachusetts Institute of Technology, Cambridge, MA 02139, USA. (hmnepf@mit.edu)

H. Andradóttir, Mars & Company, 124 Mason Street, Greenwich, CT 06830, USA. (hrund_a@yahoo.com)

(Received January 31, 2001; revised August 6, 2001;
accepted August 13, 2001.)